



sbt



5th European conference on Microfluidics  $\mu$ 'Flu18.  
Strasbourg, 28 February 2018.



## Hydrodynamic Experimental and Numerical Study of Micro-fabricated Regenerator.

PhD student (Speaker):

Tutors CEA/SBT:

Tutors LEGI:

SOCHINSKII Arkadii

LUCHIER N. (Director)

MEDRANO-MUNOZ M.

AYELA F. (Co-director)

COLOMBET D.

# Plan

## Introduction:

- Context.
- Previous works.
- Objectives.

## Numerical study:

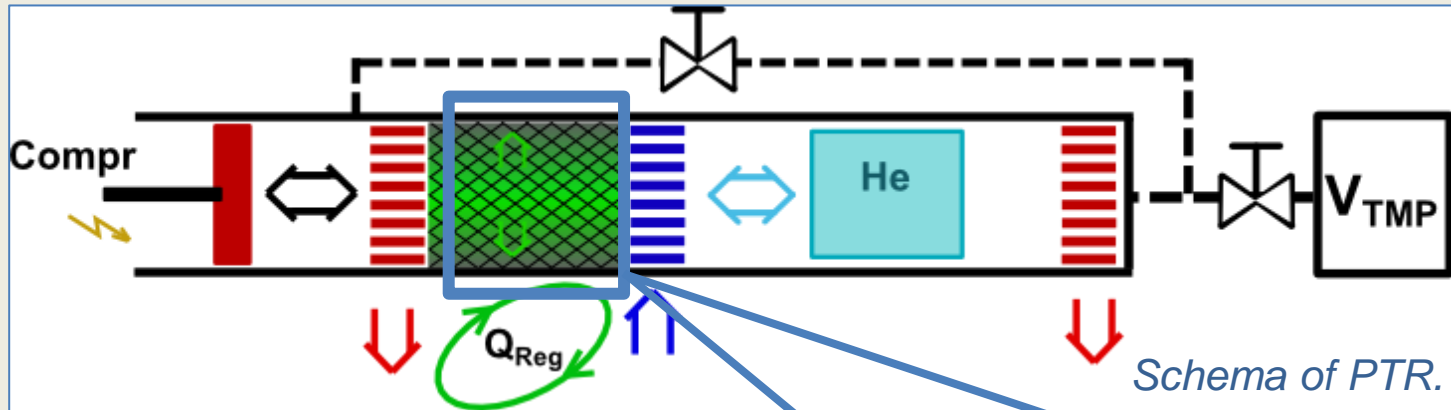
- Mesh, mathematical model and solver.
- Direct numerical simulation.
- Results and discussion.

## Experimental study:

- Micro-machining of regenerators samples.
- Experimental installation.
- Results and discussion.

## Conclusion et perspectives.

# Regenerator matrix



**Regenerators** are employed in Pulse Tube Refrigerators (PTR) or Stirling cycle machines. Its matrix is often composed of

- a) Superposed metallic lattices ( $\text{\O}30\text{-}110\ \mu\text{m}$ ) further called wound woven matrix.
- b) metallic spheres ( $\text{\O}300\ \mu\text{m}$ ).

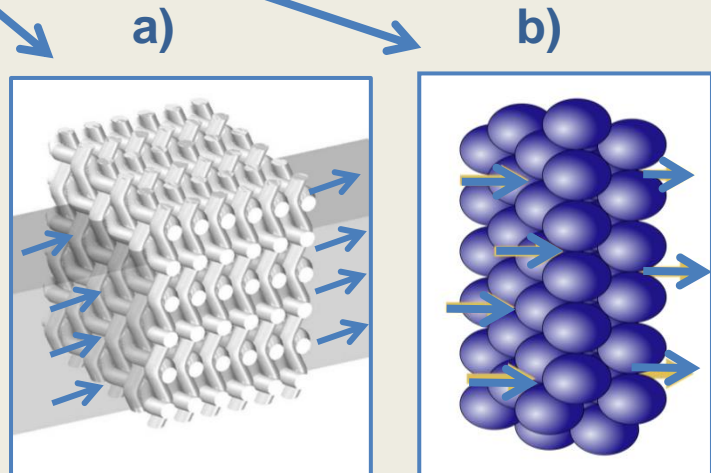


Fig. Costa(2013)\*

$$\text{Regen. Performance} = \frac{\text{Heat transfer}}{\text{Pressure losses}}$$

\*Costa(2013) – Costa S., Barrutia H., Esnaola J., Tutar M. Numerical study of pressure drop phenomena in wound woven matrix of Stirling regenerator. Energy conversion and management. 2013.

# Hydrodynamic pressure losses in traditional regenerator matrix

Friction factor  $f$  (Darcy-Weisbach) describes pressure drop losses ( $\Delta P$ ) in regenerator matrices.

Ergun(1952) gave general empirical correlation for friction factor  $f$  for stationary laminar flow in porous matrix:

$$f = 133 \cdot Re^{-1} + 2,33$$

Gedeon(1996) experimentally obtained  $f$  for stationary flow through the Regenerator's wound woven matrix (fig.) composed of metallic wires  $\varnothing 53\mu\text{m}$  with porosity  $\varepsilon = 62\%$  :

$$f = 129 \cdot Re^{-1} + 2,91 \cdot Re^{-0,103} \quad 1 < Re < 6000$$

Costa(2013) numerically obtained  $f$  for stationary flow through the Regen. wound woven matrix (fig.) of  $\varnothing 80\text{-}110\mu\text{m}$  and  $\varepsilon = 47 - 64\%$ .

$$f = 123 \cdot Re^{-1} + 3,2 \cdot Re^{-0,104}$$

$$10 < Re < 400$$

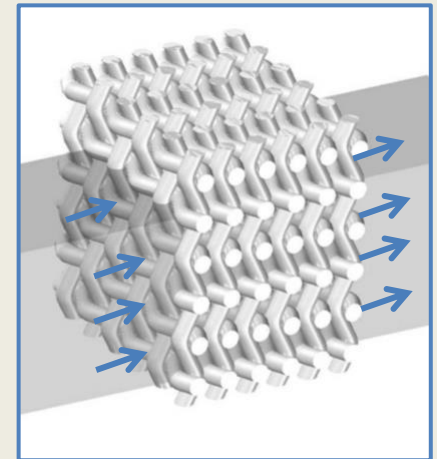
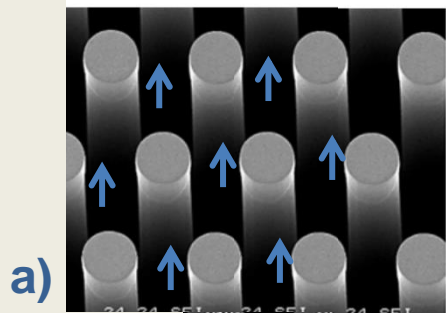


Fig. Wound woven matrix of Stirling regenerator - Costa(2013)

Optimisation and miniaturisation is complicated!

# Hydrodynamic pressure losses in micro-machined regenerator matrix



a)

Vanapalli(2007)\* studied the influence of form on a hydraulic pressure losses in a matrix of pillars etched in Si wafer. **Porosity** was fixed to  $\varepsilon = 75\%$  and **aspect ratio**  $\xi$  of opening width e and etching depth h close to  $\xi = e/h = 0,1$ .

a) Circles

$$f = 103,5 \cdot Re^{-0,44}$$

b) Sinusoidal

$$f = 29,65 \cdot Re^{-0,94}$$

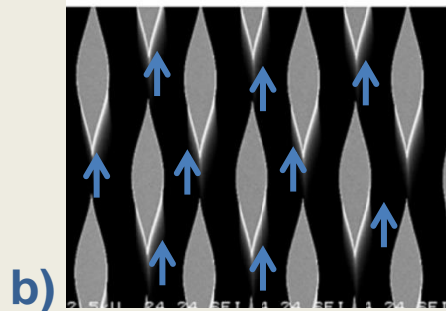
Quite optimistic!

c) Eye

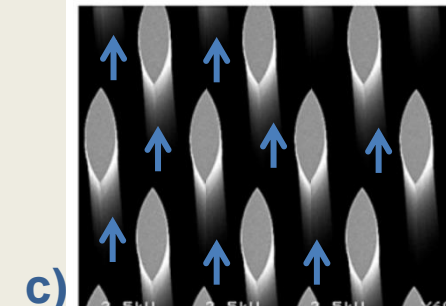
$$f = 87,10 \cdot Re^{-0,80}$$

d) Rhomboid

$$f = 175,20 \cdot Re^{-0,94}$$

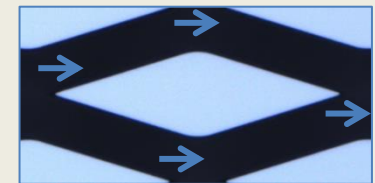


b)



c)

Objective for our study is to show influence of porosity  $\varepsilon$  on  $f$  micro-machined regenerator matrices.



d)

Fig. Vanapalli (2007)\*

\*Vanapalli(2007) – Vanapalli S., ter Brake H., Jansen H., et al. Pressure drop of laminar gas flow in a microchannel containing various pillar matrices. J. Micromech. Microeng. 2007.

# Dimensional analysis

Friction factor with :  
 $U_m$  - mean velocity.

$$f = \frac{\Delta P}{\frac{1}{2} \rho \cdot U_m^2} \frac{D_h}{L_L}$$

Reynolds numbers  
 $1 < Re < 100$ :

$$Re = \frac{U_m \cdot D_h}{\mu / \rho}$$

Hydraulic diameter with:  $S_{cont}$  - wetted surface,  $l_p$  - wetted perimeter,  $h$  - etching depth.

Porosity:

$$\varepsilon = \frac{L_L \cdot L_T - a \cdot b}{L_L \cdot L_T}$$

$$D_h = \frac{4\varepsilon V}{S_{cont}} = \frac{4\varepsilon \cdot L_L \cdot L_T \cdot h}{2l_p \cdot h + 2\varepsilon \cdot L_L \cdot L_T}$$

Length/width ratio of rhombus:

$$\alpha = \text{atan} \left( \frac{a}{b} \right) = 33^\circ$$

Aspect ratio  $\xi$  (for 2D  $\xi \rightarrow 0$ ):

$$\xi = \frac{e}{h} \sim \frac{2 \cdot L_L \cdot L_T \cdot \varepsilon}{2 \cdot l_p \cdot h}$$

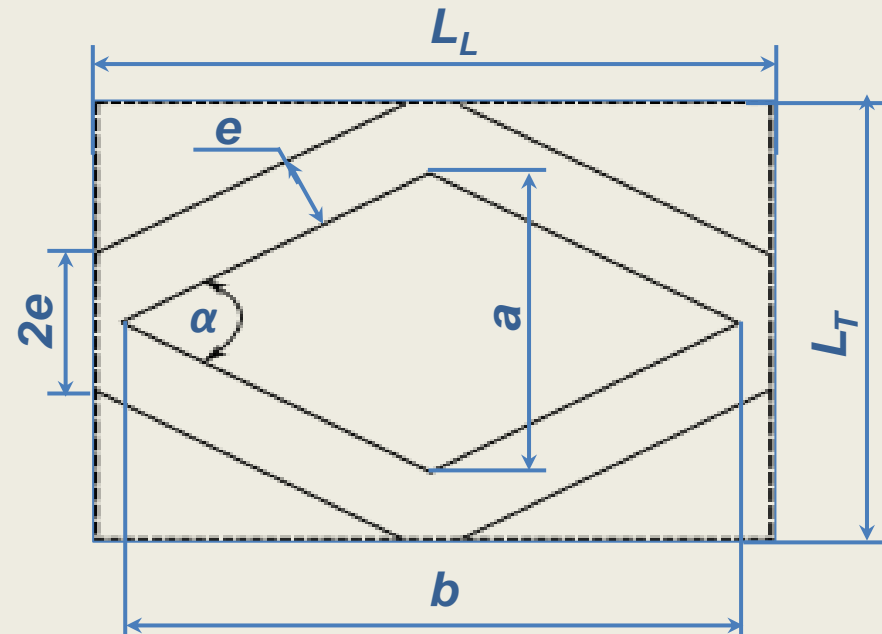


Fig. REV – Representative Elementary Volume .

# Plan.

## Introduction:

- Context.
- Previous works.
- Objectives.

## Numerical study:

- Mesh, mathematical model and solver.
- Direct numerical simulation.
- Results and discussion.

## Experimental study:

- Micro-machining of regenerators samples.
- Experimental installation.
- Results and discussion..

## Conclusion et perspectives.

# Direct Numerical Simulation (DNS)

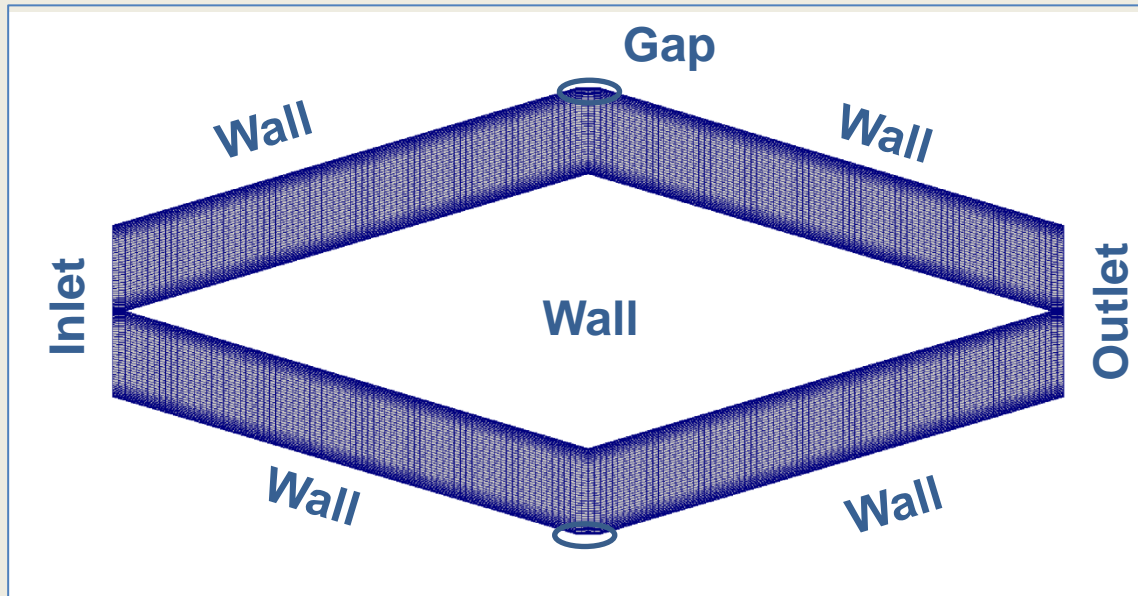
Equations for stationary incompressible flow:

$$\begin{cases} \nabla \cdot U = 0 \\ ((\nabla \cdot U)U = -\nabla \cdot p + \vartheta \cdot \nabla^2 \cdot U \end{cases} \quad \text{avec} \quad \vartheta = \frac{\mu}{\rho}$$

OpenFOAM Solver:

*simpleFoam*  
(laminar)

Linear pressure gradient is imposed to settle the flow.



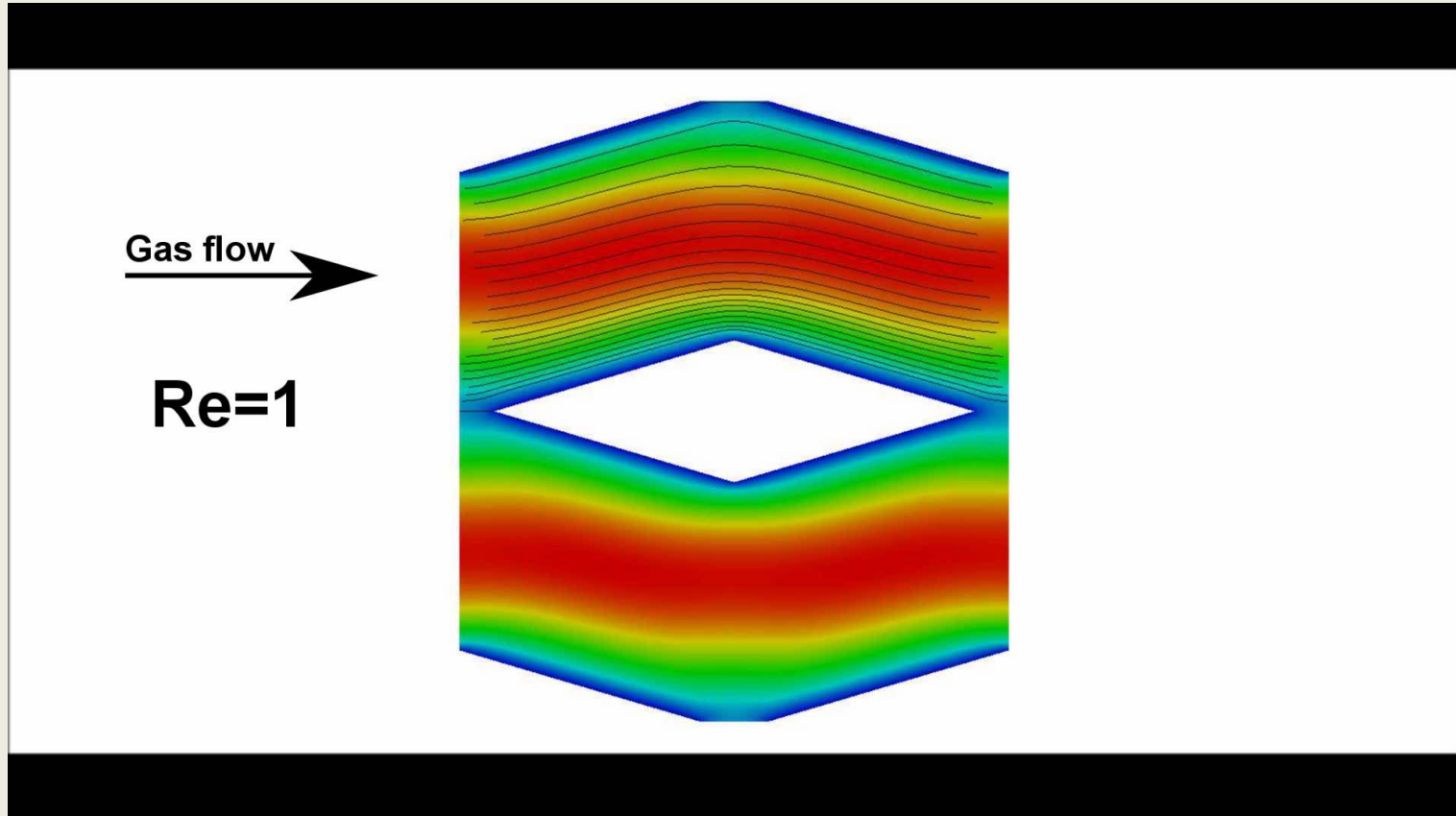
Boundary Conditions (BC):

- Inlet/Outlet: “cyclic” for pressure  $p$  and velocity  $U(x,y)$ .
- Walls:  $U(\text{wall})=0$ .
- Gap: “Symmetry plane”

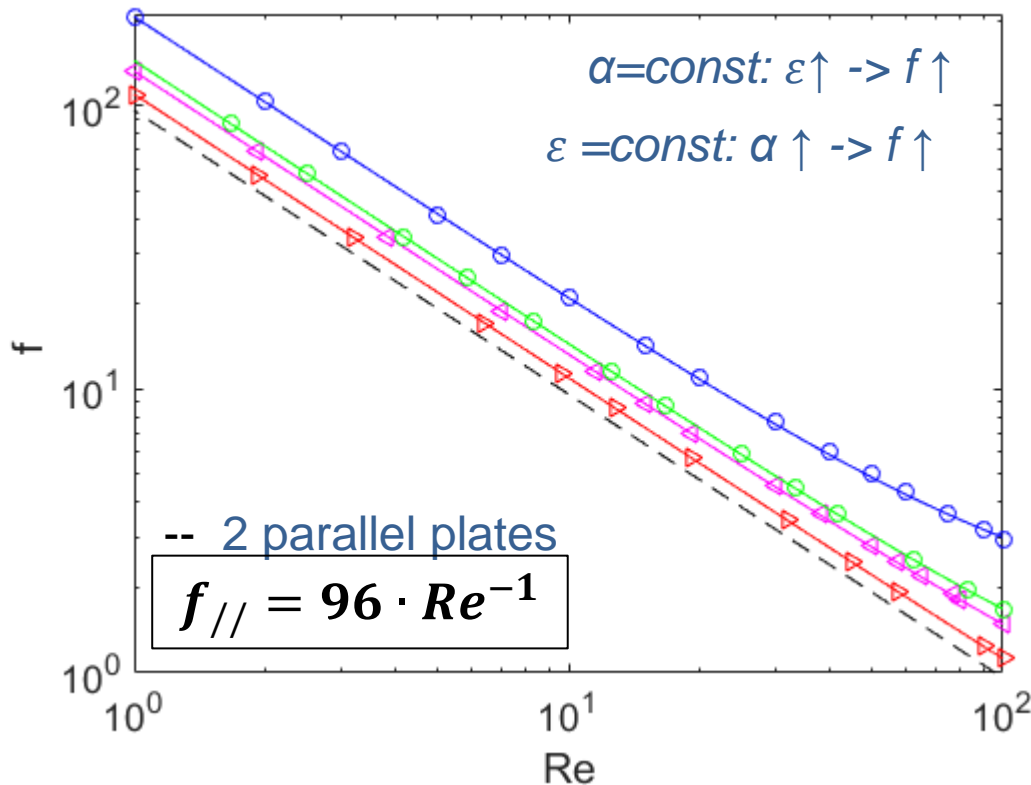
Fig. Mesh example for REV with  $\alpha=33^\circ$ ,  $\varepsilon = 40\%$  and BC imposed.



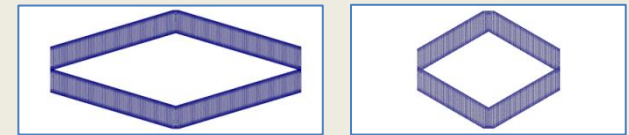
# Velocity field $U(x,y)$ for different Re DNS for REV $\alpha=33^\circ$ , $\varepsilon=80\%$



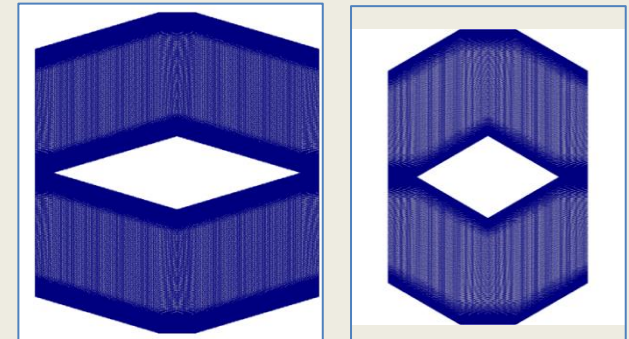
# DNS friction factor $f$ for REV with $\alpha=33^\circ$ and $60^\circ$



$\alpha=33^\circ, \epsilon=40\%, \alpha=60^\circ$



$\alpha=33^\circ, \epsilon=80\%, \alpha=60^\circ$



$\triangleright \alpha=33^\circ, \epsilon=40\%$

$$f_{\alpha=33^\circ, 40\%} = 109,6 \cdot Re^{-1}$$

$\triangleleft \alpha=33^\circ, \epsilon=80\%$

$$f_{\alpha=33^\circ, 80\%} = 132,0 \cdot Re^{-1} \cdot (1 + 2,5 \cdot 10^{-4} \cdot Re^{-1,4})$$

$\circ \alpha=60^\circ, \epsilon=40\%$

$$f_{\alpha=60^\circ, 40\%} = 143,7 \cdot Re^{-1} (1 + 2,2 \cdot 10^{-4} \cdot Re^{-1,4})$$

$\circ \alpha=60^\circ, \epsilon=80\%$

$$f_{\alpha=60^\circ, 80\%} = 205,2 \cdot Re^{-1} (1 + 12,0 \cdot 10^{-4} \cdot Re^{-1,3})$$

# Plan

## Introduction:

- Context.
- Previous works.
- Objectives.

## Numerical study:

- Mesh, mathematical model and solver.
- Direct numerical simulation.
- Results and discussion.

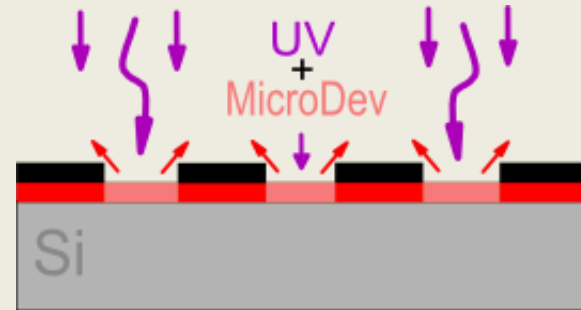
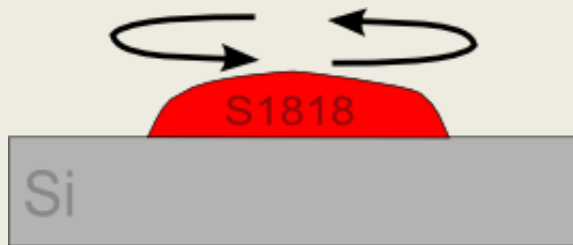
## Experimental study:

- Micro-machining of regenerators samples.
- Experimental installation.
- Results and discussion.

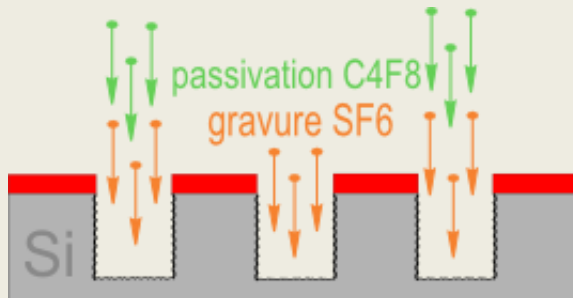
## Conclusion et perspectives.

# Micro-machining of Regenerator

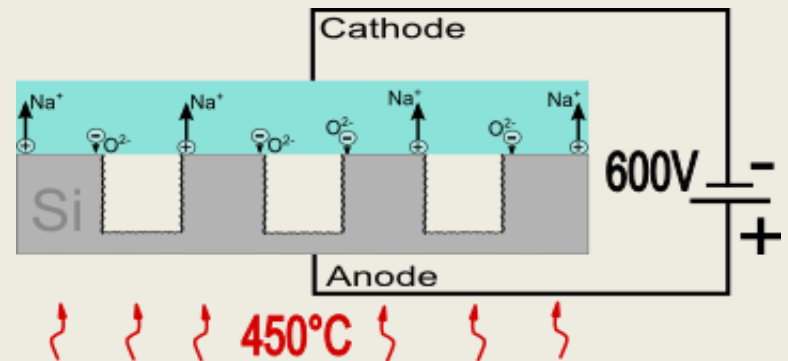
## 1. Lithography of UV polymer ( S1818 or AZ4562).



## 2. Deep Reactive Ion Etching DRIE (h=100-250µm).



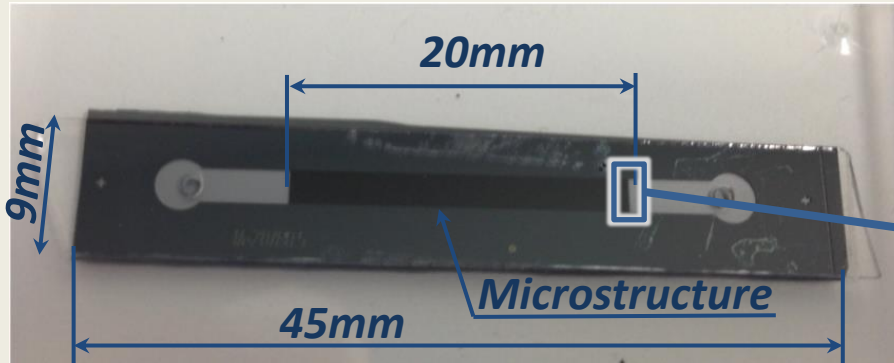
## 3. Anodic bonding with Pyrex.



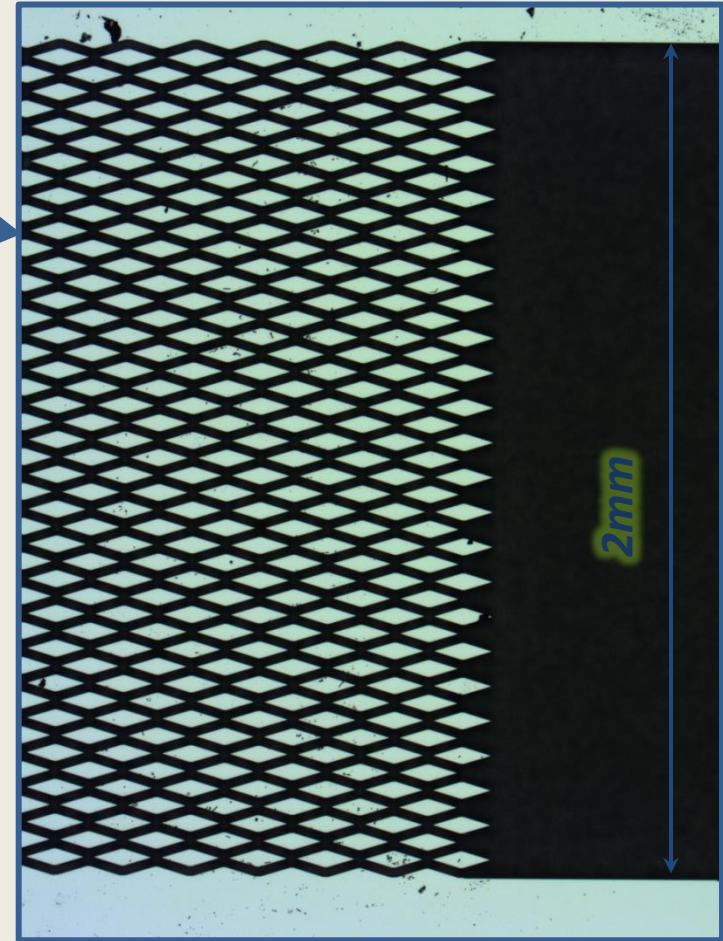
Clean rooms:

- Plateforme Technologique Amont. - NanoFab, Institut Néel.

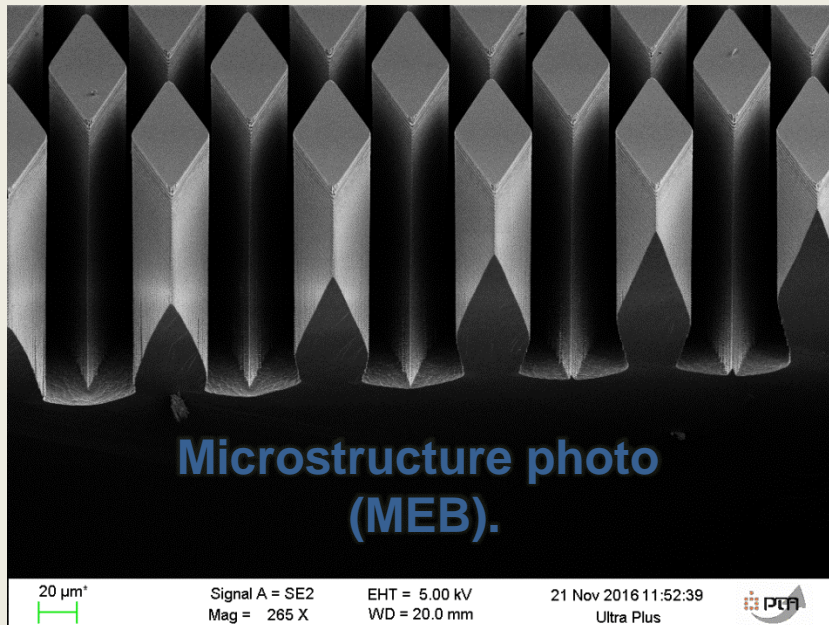
# Microstructure of regenerator



Regenerator's sample photo.



The photo of microstructure.



# Experimental test setup

$P_{in}$ ,  $P_{out}$  : pressure gauges.

$Tc_{in}$ ,  $Tc_{out}$  : thermocouples.

$Q$  – flowmeter.

$V_{tmp}$  – buffer volume.

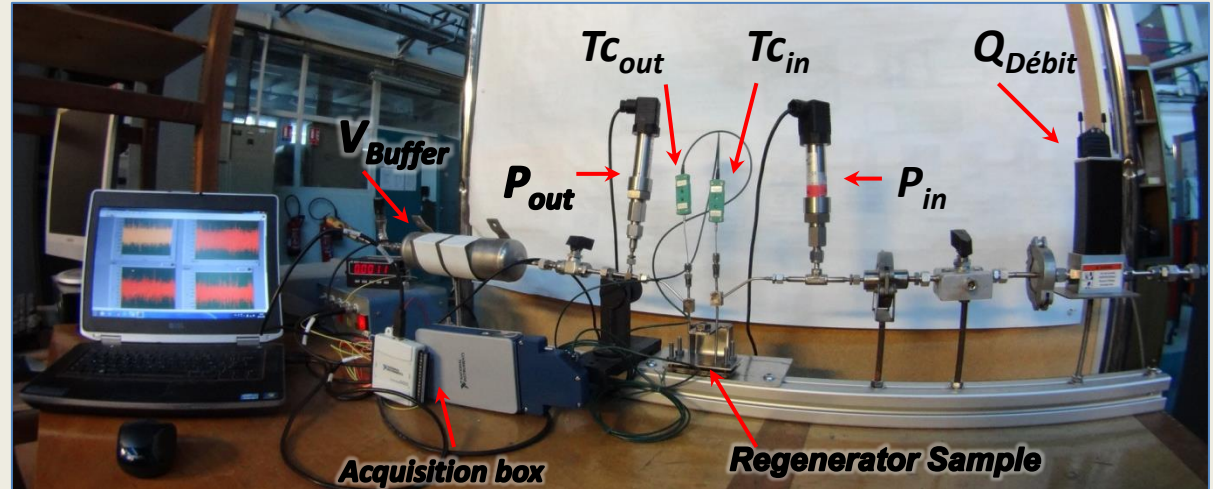


Fig. Photo of expérimental setup .

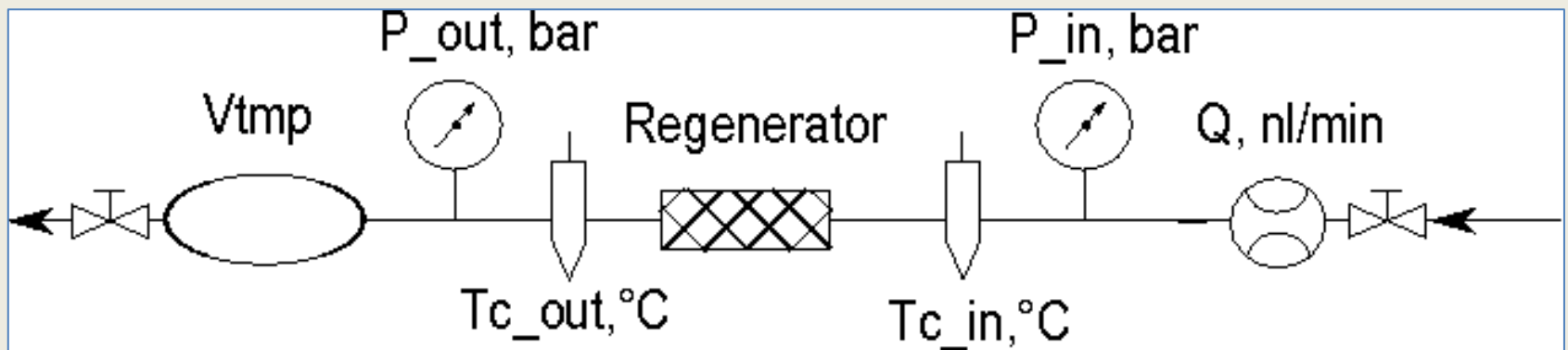
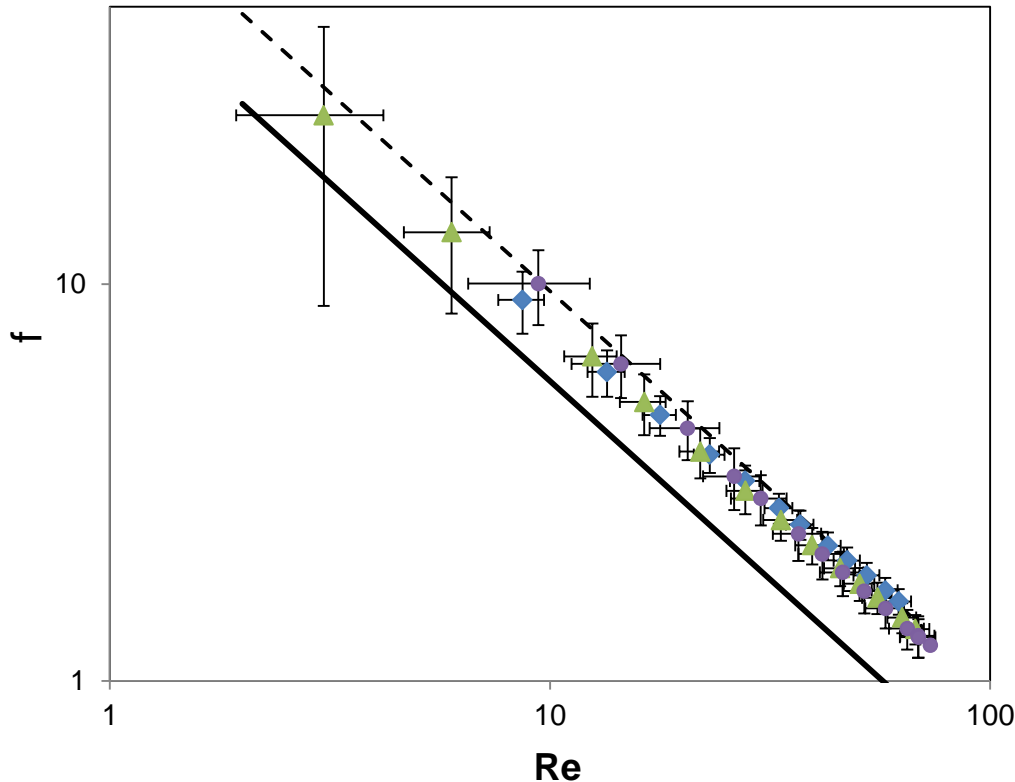


Fig. Schema for experimental measurements .

# Confirmation of experimental setup by test of empty channels



▲ Canal\_KOH02,  $h=22,4\mu\text{m}$   
 $\xi=0,011$ ,  $D_h=44,3\mu\text{m}$

$$f_{Can\_KOH2} = 84,4 \cdot Re^{-1}$$

● Canal\_KOH03,  $h=31,4\mu\text{m}$ ,  
 $\xi=0,016$ ,  $D_h=61,3\mu\text{m}$

$$f_{Can\_KOH3} = 87,2 \cdot Re^{-1}$$

◆ Canal\_KOH04,  $h=17,2\mu\text{m}$ ,  
 $\xi=0,009$ ,  $D_h=33,9\mu\text{m}$

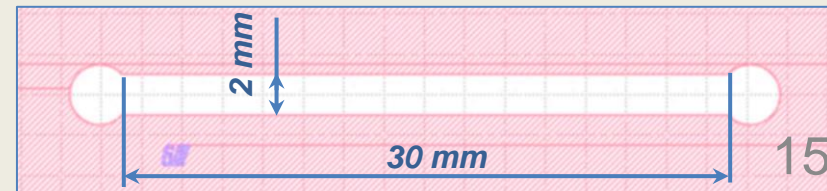
$$f_{Can\_KOH4} = 88,1 \cdot Re^{-1}$$

- Square channel  $\xi=1$

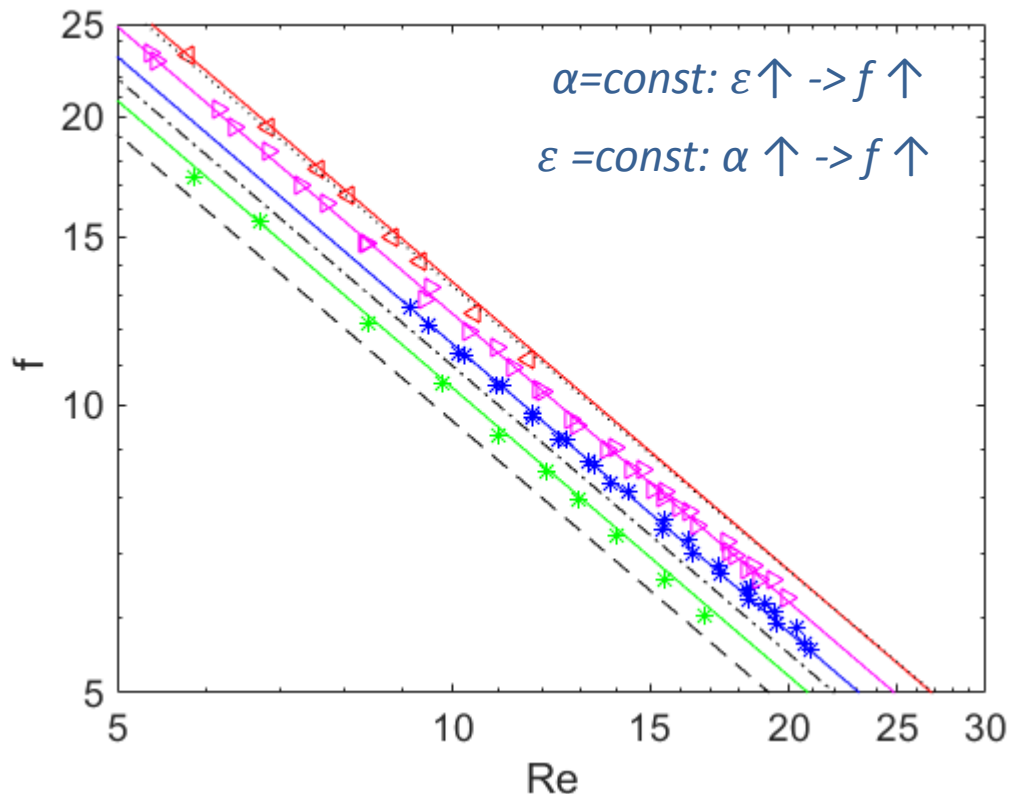
$$f_{\blacksquare} = 56,96 \cdot Re^{-1}$$

-- 2 parallel plates  $\xi=0$

$$f_{//} = 96 \cdot Re^{-1}$$



# Experimental study of regenerator's matrices with $\alpha=33^\circ$ and $e=20\mu\text{m}$



-- 2 parallel plates

-.- DNS  $\varepsilon = 40\%$ ,  $\xi = 0$ .

... DNS  $\varepsilon = 80\%$ ,  $\xi = 0$ .

$$f_{//} = 96 \cdot Re^{-1}$$

$$f_{\alpha=33^\circ, 40\%} = 109,6 \cdot Re^{-1}$$

$$f_{\alpha=33^\circ, 80\%} = 132,0 \cdot Re^{-1}$$

\* Regen2\_DR13,  
 $\varepsilon = 41,7\%$ ,  $\xi = 0,099$ ,  $D_h = 43,3\mu\text{m}$

$$f_{Reg2\_DR13} = 104,0 \cdot Re^{-1}$$

\* Regen2\_DR05,  
 $\varepsilon = 45,1\%$ ,  $\xi = 0,178$ ,  $D_h = 45,2\mu\text{m}$

$$f_{Reg2\_DR05} = 115,6 \cdot Re^{-1}$$

▷ Regen3\_DR12,  
 $\varepsilon = 65,2\%$ ,  $\xi = 0,193$ ,  $D_h = 45,3\mu\text{m}$

$$f_{Reg3\_DR12} = 124,3 \cdot Re^{-1}$$

◁ Regen3\_DR13,  
 $\varepsilon = 61,8\%$ ,  $\xi = 0,102$ ,  $D_h = 44,9\mu\text{m}$

$$f_{Reg3\_DR13} = 134,2 \cdot Re^{-1}$$



# Conclusion

## Conclusion:

- The influence of porosity  $\varepsilon$  is shown numerically and confirmed experimentally. For identical pillars, matrices with lower porosity have lower friction factor.  $\alpha = \text{const}: \varepsilon \uparrow \rightarrow f \uparrow$
- For fixed porosity  $\varepsilon$ , matrices composed of pillars with lower angle  $\alpha$  have lower friction factor.  $\varepsilon = \text{const}: \alpha \uparrow \rightarrow f \uparrow$
- The limits for friction factor  $f$  in micro-machined matrix are given by two parallel flat plates ( $f = 96/\text{Re}$ ) for aspect ratios  $\xi \rightarrow 0$  and square channel ( $f = 56,96/\text{Re}$ ) for  $\xi \rightarrow 1$ .
- Friction factor  $f$  of micro-machined regenerator's matrices with  $\alpha = 33^\circ$  and porosities  $\varepsilon < 70\%$  seems to be favorable comparing with wound woven matrices (superposed metallic wire lattices).

# Perspectives

## Perspectives:

- Implantation of resistance thermometers inside the regenerator's matrix to study the heat transfer efficiency (Nusselt number) and its dependence on porosity and pillars shape.
- Passive module of PTR etched in Si.

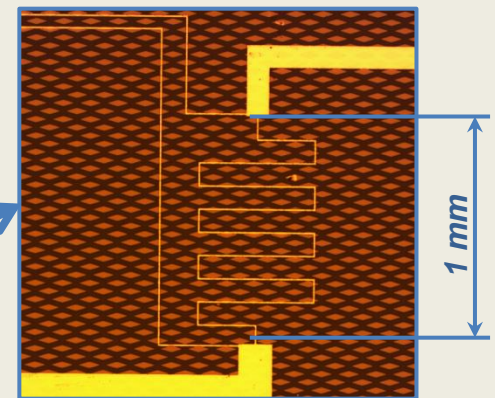
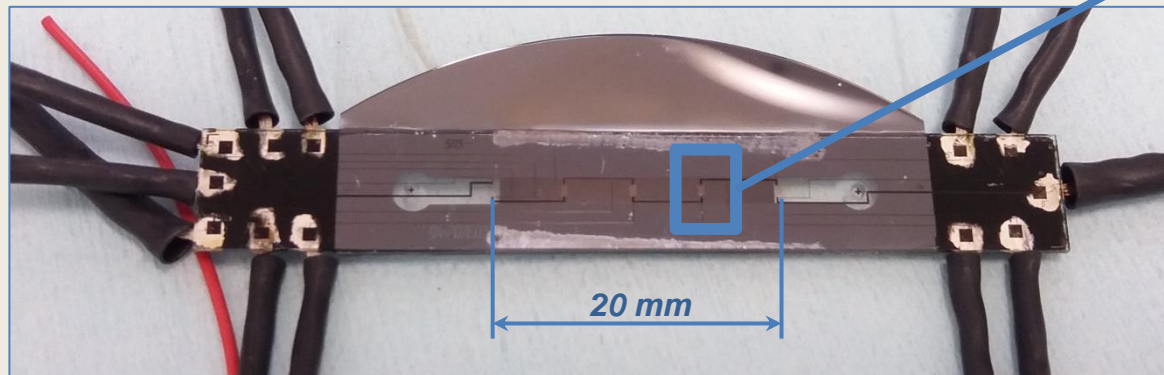


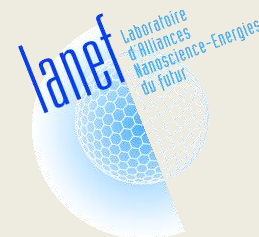
fig. Photo of micro-machined regenerator's sample equipped by thermometer .

# Thank you for your attention!

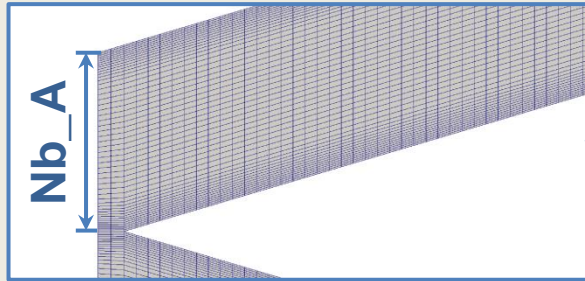
Contact speaker: [Arkadii.Sochinskii@univ-grenoble-alpes.fr](mailto:Arkadii.Sochinskii@univ-grenoble-alpes.fr)

Acknowledgments:

Labex LANEF for funding of this PhD research.

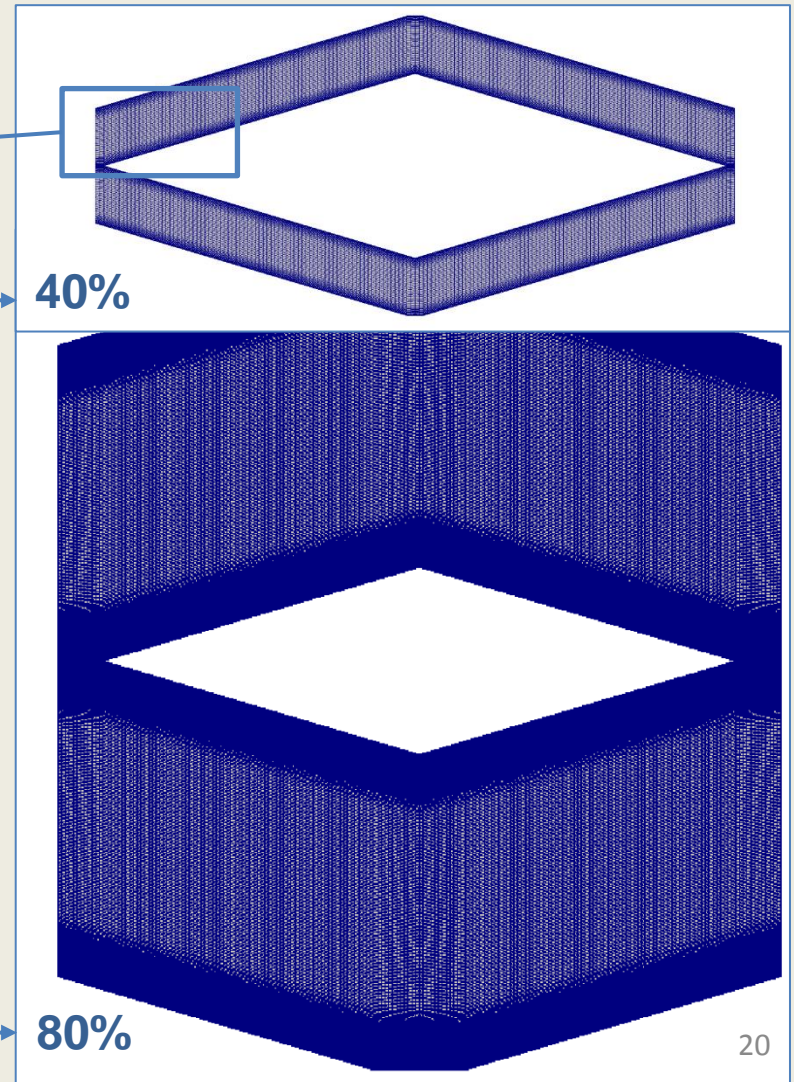


# Annexe 1: Meshing.



Mesh characteristics for  $\alpha=33^\circ$   
(number of finite volumes VF):

Mesh	Total FV	Nb_A
$\varepsilon=40\%$	16400	50
$\varepsilon=50\%$	23520	70
$\varepsilon=60\%$	35200	100
$\varepsilon=70\%$	64800	180
$\varepsilon=80\%$	96000	250
$\varepsilon=90\%$	139200	300



# Anexe2: Experimental analysis for matrices with $\alpha=33^\circ$ ; $\varepsilon=40,60\%$ ; $1 < Re < 60$ .

DNS  $\varepsilon=40\%, \xi=0$

$$f_{40\%} = 109,6 \cdot Re^{-1}$$

DNS  $\varepsilon=60\%, \xi=0$

$$f_{60\%} = 115,2 \cdot Re^{-1}$$

$e=20\mu\text{m}$

Reg2\_DR13,  $\xi=0,099$ ,  
 $\varepsilon=41,7\%$ ,  $D_h=43,3\mu\text{m}$

$$f = 104,0 \cdot Re^{-1}$$

Reg3\_DR13,  $\xi=0,102$ ,  
 $\varepsilon=61,8\%$ ,  $D_h=44,9\mu\text{m}$

$$f = 134,2 \cdot Re^{-1}$$

Reg2\_DR05,  $\xi=0,178$ ,  
 $\varepsilon=45,1\%$ ,  $D_h=45,2\mu\text{m}$

$$f = 115,6 \cdot Re^{-1}$$

Reg3\_DR12,  $\xi=0,193$ ,  
 $\varepsilon=65,2\%$ ,  $D_h=45,3\mu\text{m}$

$$f = 124,3 \cdot Re^{-1}$$

$e=40\mu\text{m}$

Reg4\_DR05,  $\xi=0,290$ ,  
 $\varepsilon=42,0\%$ ,  $D_h=73,4\mu\text{m}$

$$f = 103,9 \cdot Re^{-1}$$

Reg5\_DR05,  $\xi=0,314$ ,  
 $\varepsilon=63,8\%$ ,  $D_h=77,8\mu\text{m}$

$$f = 124,2 \cdot Re^{-1}$$

Reg7\_DR05,  $\xi=0,115$ ,  
 $\varepsilon=45,1\%$ ,  $D_h=29,5\mu\text{m}$

$$f = 107,6 \cdot Re^{-1}$$

Reg5\_DR12,  $\xi=0,333$ ,  
 $\varepsilon=62,0\%$ ,  $D_h=72,8\mu\text{m}$

$$f = 133,3 \cdot Re^{-1}$$

$e=10\mu\text{m}$

Reg7\_DR13,  $\xi=0,088$ ,  
 $\varepsilon=46,0\%$ ,  $D_h=26,4\mu\text{m}$

$$f = 113,7 \cdot Re^{-1}$$

Reg8\_DR05,  $\xi=0,131$ ,  
 $\varepsilon=65,2\%$ ,  $D_h=33,2\mu\text{m}$

$$f = 116,4 \cdot Re^{-1}$$

DNS  $\varepsilon=50\%, \xi=0$

$$f_{50\%} = 111,6 \cdot Re^{-1}$$

DNS  $\varepsilon=70\%, \xi=0$

$$f_{70\%} = 121,0 \cdot Re^{-1}$$